

Analytical Study of Combined Convection Heat Transfer for Flow in a Horizontal Annulus

Ahmed .J. Shkarah

Mechanical Eng. Dept.
College of Engineering
Thi-Qar University

Mushtaq .I. Hasan

Mechanical Eng. Dept.
College of Engineering
Thi-Qar University

Iqbal .K. Eraebee

Civil Eng. Dept.
College of Engineering
Thi-Qar University

Abstract

In this paper a numerical investigation is made to study the axially symmetric, laminar air flow in the entrance region of an annulus by solving the two dimensional governing equations of motion (continuity, momentum & energy) using implicit finite difference method and the Gauss elimination technique. A STAR CCM + program is used. The results obtained for velocity and temperature profile revealed that, the secondary flow created by natural convection have a significant effect on the heat transfer process. A comparison has been made for results which show a good agreement.

Keywords: numerical combined convection; thermally developing flow; finite difference; horizontal annulus.

المستخلص

في هذا البحث تم دراسة عملية انتقال الحرارة خلال انبوبي متحدي المركز في منطقة الدخول عددياً من خلال حل معادلات الحركة (معادلة الاستمرارية ، معادلة الزخم ومعادلة الطاقة) ثنائية الابعاد باستخدام طريقة الفروقات المحددة وطريقة كاوس للحذف باستخدام برنامج (STAR CCM). النتائج التي تم الحصول عليها فيما يخص السرعة ودرجة الحرارة تشير إلى أن الجريان الثانوي المتولد بواسطة الحمل الحر له تأثير مهم على عملية انتقال الحرارة . تم مقارنة النتائج ووجد أن هناك تقارب جيد.

1. Introduction

Convection heat transfer is one of the important heat transfer modes, this process is classified into three distinct types (natural, forced and mixed) convection. The interaction of the natural and forced convection currents can be very complex and difficult because it depends not only on all the parameters determining both forced and free convection relative to

one another but sometimes also on a large number of interacting parameters including the relative direction of the natural and forced convection to each other, the arrangement of the geometry, the velocity profile at annulus entrance and the heating surface boundary conditions [2]. Laminar flow combined convection heat transfer in annulus is encountered in a wide variety because of special importance in many industrial engineering applications. The following examples can be cited: heating or cooling of double pipe heat exchangers for viscous liquids, heat exchangers for gas flows [2], cooling of electronic equipment, compact heat exchangers [3], and the cooling core of nuclear reactors [4]. The full understanding of the prevailing velocity and temperature fields, as well as, the pressure drop and heat transfer coefficient, is necessary for the proper design. In addition, to estimate the magnitude of the thermal shock that any one of the preceding systems wall will suffer [5, 6, 7].

Therefore, considering the secondary flow motion continues along the annulus, where as in the uniform inner wall temperature boundary condition, the secondary flow motion develops to a maximum intensity and then diminishes to zero as the temperature difference continuously decreases [8, 9, and 10].

2. Mathematical modeling

2.1. Governing equations

The governing equations of motion are developed on the following assumptions:

Fully developed velocity profile at the entrance of the test section, Steady state laminar and upward flow, Constant wall heat flux at annulus inner tube, constants fluid properties except the density in the buoyancy term and viscous dissipation is neglected.

The following Non dimensional differential equations represent conservation of continuity, momentum (Navier Stokes equations in both axial and radial directions) and energy equation [1] & [4].

Continuity equation:

$$\frac{\partial U}{\partial X} + \frac{V}{R} + \frac{\partial V}{\partial R} = 0 \quad (1)$$

Momentum equation in axial direction:

$$V \frac{\partial U}{\partial R} + U \frac{\partial U}{\partial X} = - \frac{\partial P}{\partial X} + \frac{1}{Re^2} \{ G.Cc_4 + T [Cc_5 + Cc_6 T] \} \\ + \frac{1}{Re} \left\{ [Cc_1 + T(Cc_2 + Cc_3 T)] \left[\frac{\partial^2 U}{\partial X^2} + \frac{1}{R} \frac{\partial U}{\partial R} + \frac{\partial^2 U}{\partial R^2} \right] \right\} +$$

$$\frac{1}{\text{Re}} \left\{ [C_{c_2} + 2C_{c_3}T] \left[2 \frac{\partial T}{\partial X} \cdot \frac{\partial U}{\partial X} + \frac{\partial T}{\partial R} \left(\frac{\partial V}{\partial X} + \frac{\partial U}{\partial R} \right) \right] \right\} \quad (2)$$

Momentum equation in radial direction:

$$\begin{aligned} V \frac{\partial V}{\partial R} + U \frac{\partial V}{\partial X} &= - \frac{\partial P}{\partial R} + \frac{1}{\text{Re}} [C_{c_1} + T(C_{c_2} + C_{c_3}T)] \\ * \left[\frac{\partial^2 V}{\partial X^2} + \frac{1}{R} \frac{\partial V}{\partial R} - \frac{V}{R^2} + \frac{\partial^2 V}{\partial R^2} \right] &+ \frac{1}{\text{Re}} [C_{c_2} + 2C_{c_3}T] * \\ \left\{ \left[2 \frac{\partial T}{\partial R} \cdot \frac{\partial V}{\partial R} + \frac{\partial T}{\partial X} \left(\frac{\partial V}{\partial X} + \frac{\partial U}{\partial R} \right) \right] \right\} & \quad (3) \end{aligned}$$

Energy equation:

$$V \frac{\partial T}{\partial R} + U \frac{\partial T}{\partial X} = \frac{1}{\text{Re.Pr}} \left(\frac{\partial^2 T}{\partial X^2} + \frac{1}{R} \frac{\partial T}{\partial R} + \frac{\partial^2 T}{\partial R^2} \right) \quad (4)$$

Integral continuity equation:

$$\frac{1}{2} (1 - N^2) = \int_N^1 R U \, dR \quad (5)$$

The viscosity and density variation with temperature are taken to be [11, 12, and 13]:

$$\mu = \mu_i (C_1 + C_2 t - C_3 t^2) \quad (6)$$

$$\rho = \rho_i (C_4 - C_5 t + C_6 t^2) \quad (7)$$

Where C_1, C_2, \dots, C_6 are constants.

Where the following dimensionless parameters are used:

$$U = \frac{u}{u_i}, \quad V = \frac{v}{u_i}, \quad R = \frac{r}{r_2}, \quad X = \frac{x}{r_2}, \quad p = \frac{P - P_i}{\rho_i u_i^2}, \quad T = GC_5(t - t_i), \quad N = \frac{r_1}{r_2}$$

Viscosity and density variation, equations (6, 7) in dimensionless form becomes:

$$\mu = \mu_i (C_{c_1} + C_{c_2}T - C_{c_3}T^2) \quad (8)$$

$$\rho = \rho_i (C_{c_4} - (C_{c_5}/G)T + (C_{c_6}/G)T^2) \quad (9)$$

Where:

$$\begin{aligned} C_{c_1} &= C_1 + C_2 t_i - C_3 t_i^2, \quad C_{c_2} = (1/G.C_5) (C_2 - 2C_{3i}), \quad C_{c_3} = -C_3/G^2 . C_5^2 \\ C_{c_4} &= (C_4 - C_5 t_i + C_6 t_i^2), \quad C_{c_5} = (2C_6 t_i / C_5) - 1, \quad C_{c_6} = C_6 / G . C_5^2 \end{aligned}$$

The boundary conditions in dimensionless form are:

$$\text{at } x = 0 \quad U = \frac{2}{M} (1 - R^2 + B \ln(R)), \quad B = \left(\frac{R^2 - 1}{\ln(R)} \right), \quad M = 1 + \frac{1}{N^2} - B, \quad V = 0, \quad P = 0, \quad T = 0$$

$$\text{at } R=N \text{ (for all } x), U=0, V=0, \quad q = k \left(\frac{\partial T}{\partial R} \right)_{R=N} \left(\frac{v^2}{r_2^4 C_5 g} \right) = \text{constant inner wall heat}$$

$$\text{flux. at } R=1 \text{ (for all } x), U=0, V=0$$

3. Numerical solution

In thermal entrance region, the problem of air flow with constant physical properties except the density in buoyancy term is that the energy equation (4) is coupled with the continuity and momentum equations (1 - 3). This leads to say that the problem may be divided into two parts. The equation of energy can be solved to determine the temperature profile after which the continuity equation and momentum equation can be solved to determine the hydrodynamic characteristics of the entry length by using the temperature profile previously obtained from thermal calculations. In the following numerical approximation method, the energy equation will be solved by a direct implicit technique and the hydrodynamic part of the problem will be solved by means of extension to the linearized implicit finite difference technique. A rectangular grid was used with suffices \underline{n} and \underline{m} for the axial and radial directions, respectively. A uniform radial spacing was used, but the marching procedure permitted a doubling of the axial step size at arbitrary location and any number of times. Basically, the unknown solution grid point is defined by suffix (n+1,m) and the finite difference method is used to give sets of linear equations for the variable U, V, P and T at the unknown axial position "n+1". Where the product of two unknowns occurs, linearity in the set of equations is achieved by putting one unknown of its value at the previous known step "n".

The boundary conditions in finite difference form become:

$$1. \text{ Entry condition: } U_{1,m} = \frac{2}{M} \left(1 - R^2 + B \ln(R) \right), \quad V_{1,m} = 0, \quad P_{1,m} = 0, \quad T_{1,m} = 0$$

$$2. \text{ Wall flow condition: } U_n, M_{n+1} = 0, \quad V_n, M_{n+1} = 0$$

$$3. \text{ Wall thermal condition: } T_{n,H+1} = T_{n,H} + \frac{q r_1^4 C_5 g}{v^2 S k}$$

4. Computational method and simulation program

In the present theoretical work a computational model is used to study the effect of various parameters such as the heat flux and the Reynolds number on the velocity and temperature profiles and on the heat transfer coefficient in a horizontal annulus. The procedure used to solve the above equation was as follows:

Equation (4) (for temperature) was written for each radial position at first axial step. This gives a set of $M-1$ equations for the unknowns T 's that were solved by Gauss elimination method. Then equations (1 - 3) with integral continuity equation (4) were similarly written and solved for the unknowns U , V and P and these gave equations for U , V , and P unknowns. The known values of T , U , V and P were then used as input data to solve the next axial step.

The introduction of second derivative of velocity and temperature in the axial direction means that three axial positions were involved in the finite difference approximation, two positions (suffices " $n-1$ " and " n ") were known and one (suffice " $n+1$ ") was unknown. After solution of a given step, the old values at " n " and " $n+1$ " became the new values at " $n-1$ " and " n " respectively and old " $n-1$ " data redundant, and we use STAR CCM+ package for solving problem. Knowing the temperature profiles from the numerical solution of energy, the mixing cup temperature and the local Nusselt number at any cross section can be calculated. The mixing cup temperature at any cross section is defined by:

$$t_m = \frac{\int_{r_1}^{r_2} \dot{t} u r dr}{\int_{r_1}^{r_2} \dot{u} r dr} \quad (10)$$

or, in dimensionless form:

$$T_m = \frac{\int_0^1 \dot{T} U R dR}{\int_0^1 \dot{U} R dR} \quad (11)$$

The local Nusselt number at any cross section is defined by:

$$Nu_x = \frac{qD}{k(t_{sx} - t_{mx})} \quad (12)$$

$$\text{or, in dimensionless form: } Nu_x = \frac{h_c \frac{\pi D_o \Delta T}{\dot{Q}}}{T_{sx} - T_{mx}} \quad (13)$$

Where:

T_{sx} = Dimensionless local inner tube surface temperature.

T_{mx} = Dimensionless local mixing cup temperature.

5. Results and discussion

The numerical study has been conducted mainly to study combined convection heat transfer to assisting airflow in a heated horizontal annulus. The temperature profile, velocity profile, variation of the inner tube surface temperature, and local Nusselt number along the annulus has been investigated.

5.1. Temperature profile

Generally, the variation of the surface temperature along the annulus inner tube may be affected by many parameters such as heat flux, flow velocity, the annulus inclination and the flow entrance situation.

The temperature distribution in the horizontal annulus for selected runs is plotted in Figures (1, 2). From this figure it can be seen at test section entrance the inner tube surface temperature gradually increases up to a specific axial position the temperature reaches a maximum value, after that the inner tube surface temperature decreases at annulus exit. Figure (1) shows the effect of Reynolds number on the inner tube surface temperature for heat flux (241 W/m²). It is obvious that the increase of Re lead to reduce the inner tube surface temperature, as the heat flux is kept constant. It is necessary to mention that as heat flux increases the inner tube surface temperature increases because the free convection is the dominating factor in the heat transfer process. Figure (2) shows the variation of the surface temperature along the annulus inner tube for different heat flux, for Re=598 and for calming section length equal to 60 cm ($L/D_h = 13.95$). This figure reveals that the inner tube surface temperature increases at annulus entrance reaching a maximum value after which the inner tube surface temperature decreases earlier for higher heat flux. This can be attributed to the development of the thermal boundary layer faster due to buoyancy effect as the heat flux increases for the same Reynolds number.

The inner tube surface temperature variation for the second calming section with length equal to 90 cm ($L/D^h = 20.93$) for $Re=598$, shows a similar trend as mentioned above for ($L/D^h = 13.95$).

5.2 Velocity profile

The velocity profiles along the horizontal annulus, for $Re=1200$ and for different rates of heat flux for inner wall, are shown in Figures (3 & 4), from these figures one can see that, for high (Re) number the profiles have revealed a small effect of buoyancy forces in all the profiles and show a profile similar to pure forced convection behavior. The maximum velocity occurs at dimensionless radial distance (R) equal to (17). Figure (5) shows the axial velocity profiles for $Re=540$ and for heat flux equal to 288 W/m^2 . The profile at annulus entrance ($x=0$) computed and depicted for a fully developed pure forced convection.

5.3. Surface temperature

The inner tube surface temperature distribution along a horizontal annulus is shown in Figures (7 to 9). The inner tube surface temperature distribution along the annulus, for different heat flux and for constant Reynolds numbers (332 and 1128) is shown in Figures (6&7) respectively. The temperature variation for different Reynolds numbers and for constant heat flux (82.778 W/m^2 and 545 W/m^2) is shown in Figures (8&9) respectively. The figures show that the inner tube surface temperature increases as the heat flux increases for same Reynolds number. While the inner tube surface temperature decreases as the Reynolds numbers increase for same heat flux.

5.4. Local Nusselt number (Nu_x)

The variation of local Nusselt number (Nu_x) with dimensionless axial distance (Z^+), for horizontal position is shown in Figures (10 to 13) for selected runs. The general shape of these curves plotted on a semi logarithmic plot decreases, at annulus entrance until it reaches a minimum value after which (Nu_x) increases at annulus exit. It is clear that as Z^+ approaches zero the (Nu_x) must approach infinity since at Z^+ equal to zero, the boundary layer thickness is zero.

Figures (10&11) show the effect of the heat flux variation on (Nu_x) distribution for $Re=598$ and $Re=1128$ respectively. It is clear from these two figures that at the higher heat flux, the values of (Nu_x) were slightly higher than the values of lower heat flux. This may be attributed to the secondary flow superimposed on the forced flow effect increases as the heat flux increases leading to higher heat transfer coefficient. The smooth curve in each figure represents the theoretical pure forced convection (TPFC) based on constant property analysis of [10].

Figures (12&13) shows the effect of Reynolds number variation on (Nu_x) distribution with (Z^+) , for heat flux (241 W/m^2) in Figure (12) and for high heat flux (545 W/m^2) in Figure (13). For constant heat flux, the (Nu_x) value gives higher results than the predicted pure forced convection value and moves toward the left of (TPFC) as Reynolds number increases. This situation reveals that the forced convection is dominant on the heat transfer process with little effect of buoyancy force for high Reynolds number. As the (Re) number reduced, the buoyancy effect expected to be higher which improves the heat transfer results.

It is necessary to mention that for horizontal annulus, the effect of secondary flow is high, hence at low Reynolds number and high heat flux, the situation makes the free convection predominant. Therefore, as the heat flux increases, the fluid near the inner tube wall becomes warmer and lighter than the bulk fluid in the annulus while the fluid near the outer tube (unheated) becomes heavier than the bulk fluid in the annulus. As a consequence, two upward currents flow along the inner tube circumference, and by continuity, the fluid near the inner surface of outer tube flows downward. This sets up an expected two longitudinal vortices, which are symmetrical about an inner tube. These vortices reduce the temperature difference between the inner tube surface and the air flow which lead to increase the growth of the thermal boundary layer along the annulus and causes an improvement in the heat transfer results. But at low heat flux and high Reynolds number the situation makes the forced

convection predominant and the vortices strength diminished which allow the forced flow to decrease the temperature difference between the inner tube surface and the air, hence the (Nu_x) values become higher.

The (Nu_x) distribution for the second calming section ($L/D_h=20.93$), and mentioned above when ($L/D_h=13.95$) in horizontal position, for the same Reynolds number and same heat flux.

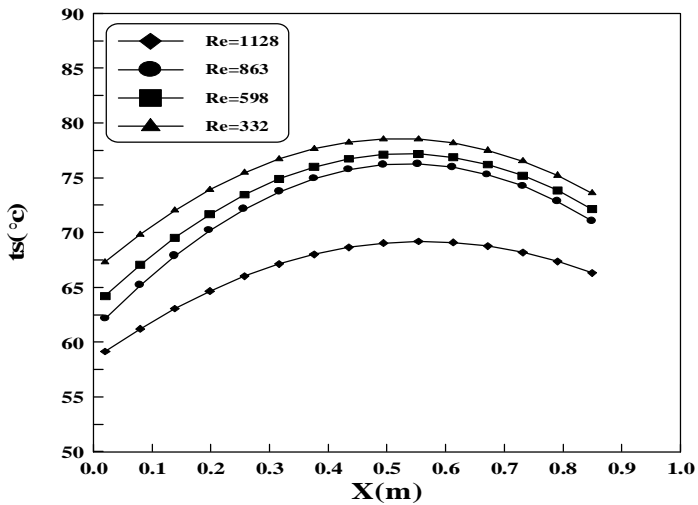
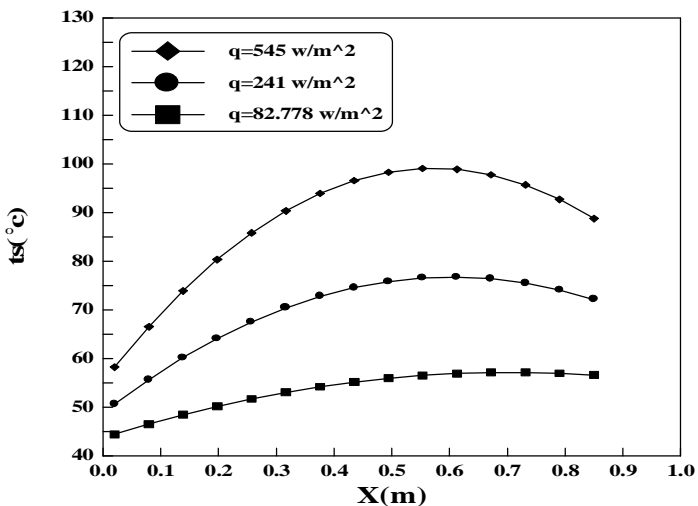
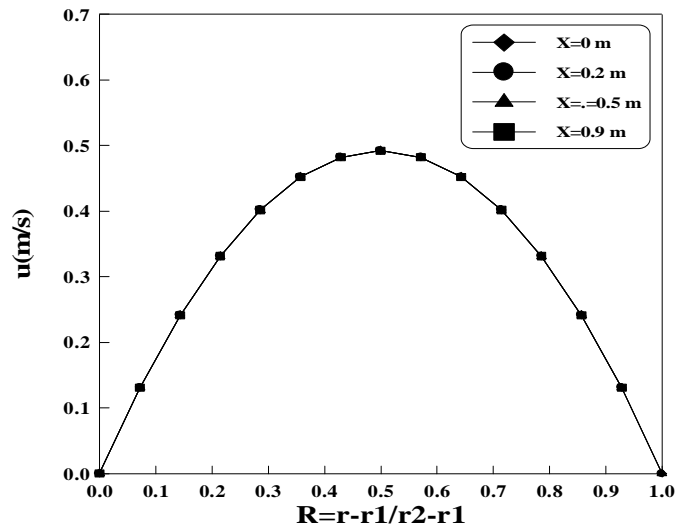


Figure (1). Variation of the inner tube surface temperature with the axial distance for $q=241 \text{ W/m}^2$, $L_{calm.}=60, q = 0^{\circ}$ (Horizontal).



Figure(2). Variation of the inner tube surface temperature with the axial distance for $Re=598, L_{calm.}=60 \text{ cm}$, $q = 0^{\circ}$ (Horizontal).



Figure(3). Developing velocity profiles along the annulus for $q=0 \text{ w/m}^2$ and $Re=1200$.

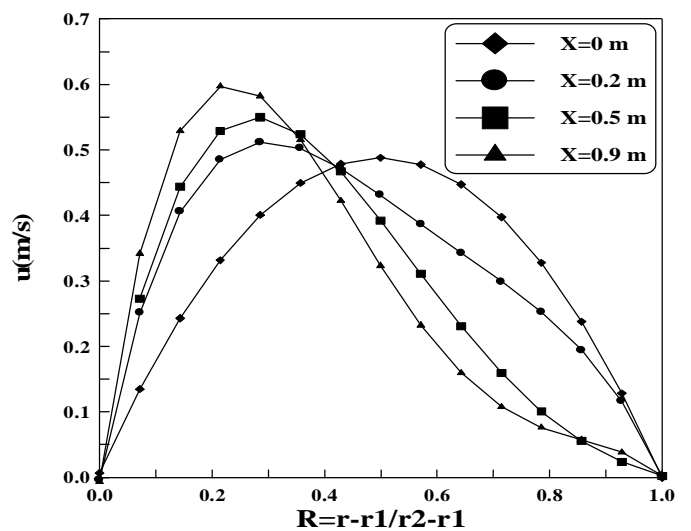


Figure (4). Developing velocity profiles along the annulus for $q=90 \text{ w/m}^2$ and $Re=1200$.

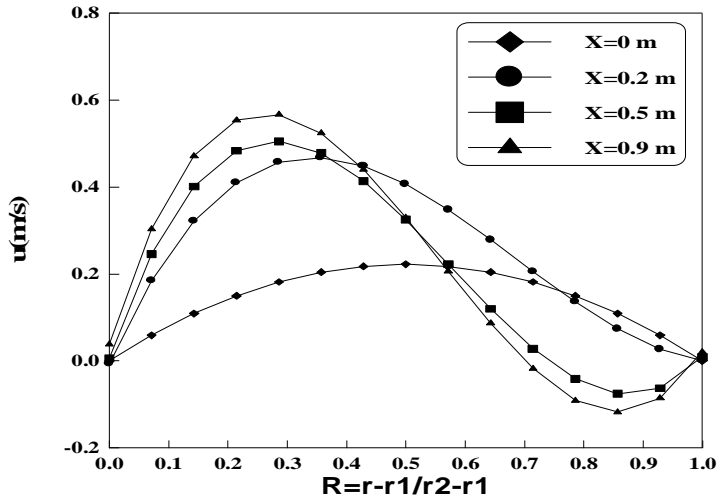
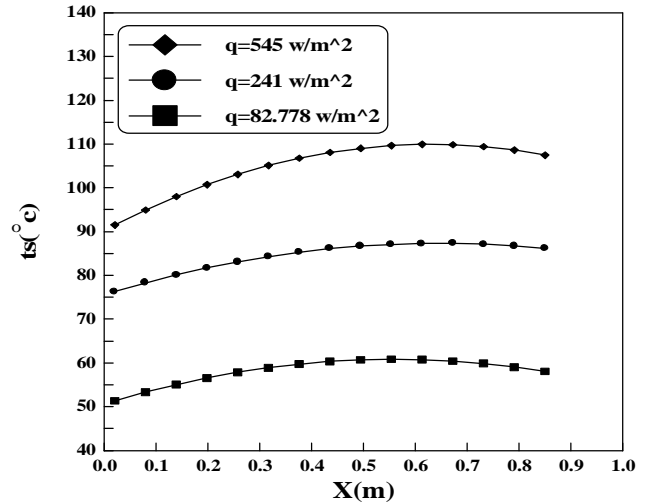


Figure (5). Developing velocity profiles along the annulus for $q=288 \text{ w/m}^2$ and $Re=540$.



Figure(6). Variation of the inner tube surface temperature along the axial distance for $Re = 332$.

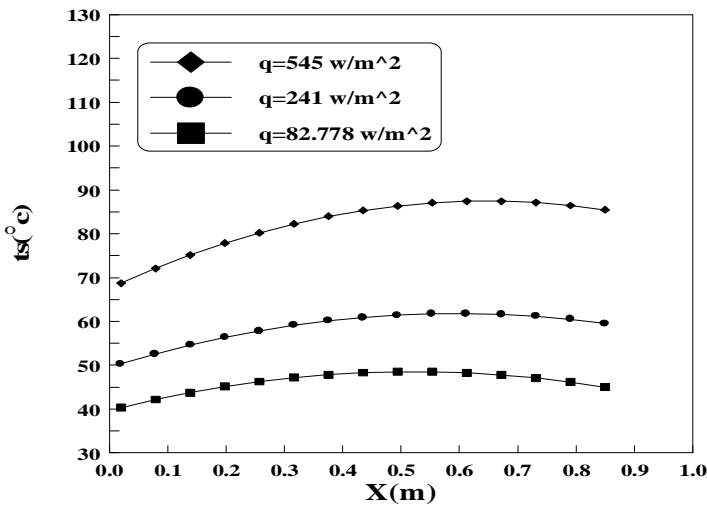


Figure (7). Variation of the inner tube surface temperature along the axial distance for $Re=1128$.

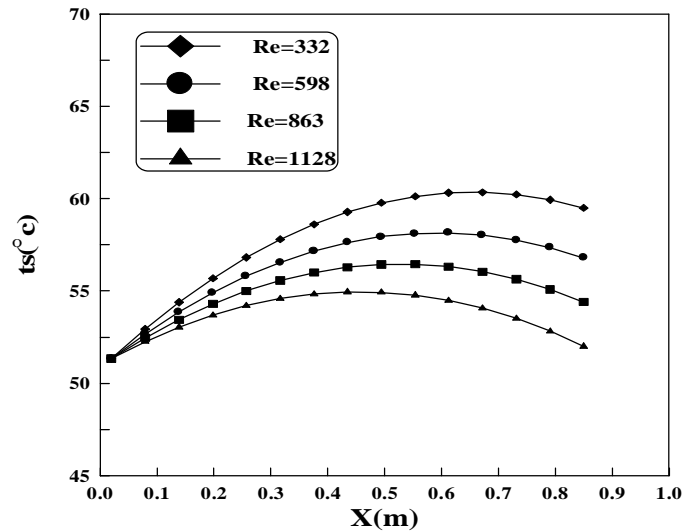


Figure (8) .Variation of the inner tube surface temperature along the axial distance for $q = 82.77 \text{ w/m}^2$.

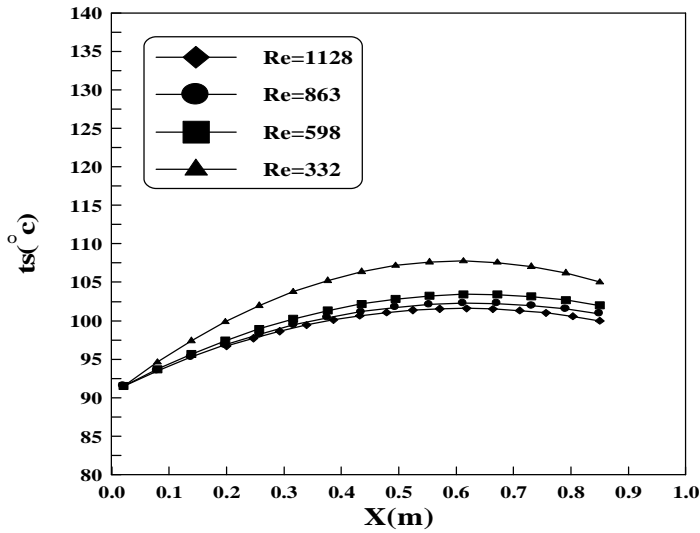


Figure (9). Variation of the inner tube surface temperature along the axial distance for $q=545 \text{ w/m}^2$.

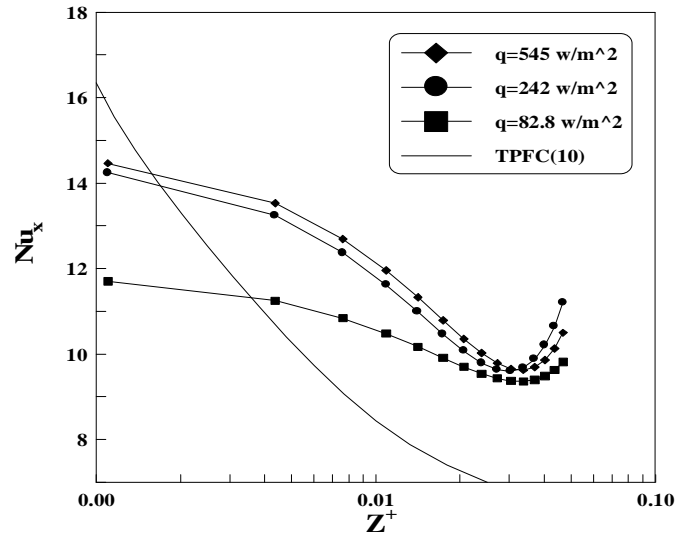


Figure (10). Variation of local Nusselt number with dimensionless axial distance for $Re = 598$, $L_{calm.} = 60 \text{ cm}, q = 0^\circ$ (Horizontal).

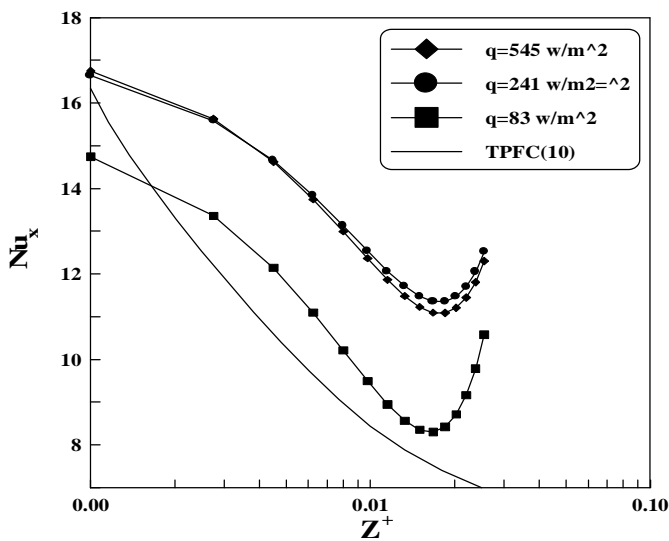


Figure (11). Variation of the local Nusselt number with dimensionless axial distance for $Re = 1128$, $L_{calm.} = 60 \text{ cm}, q = 0^\circ$ (Horizontal).

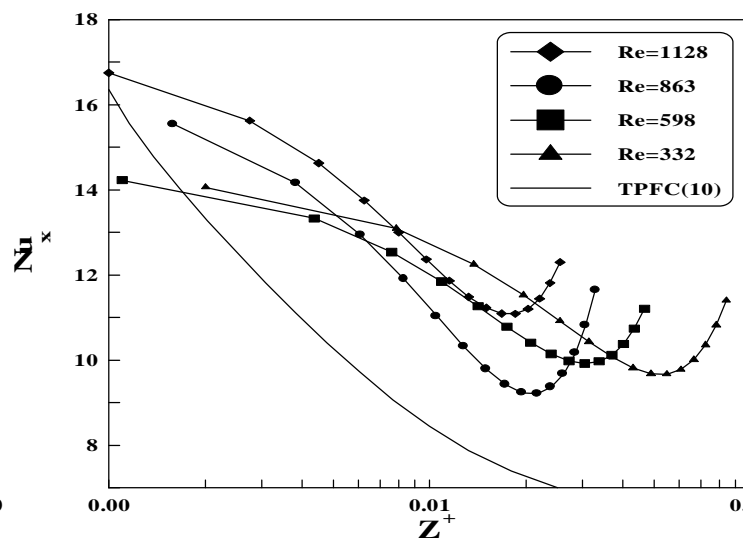


Figure (12). Variation of the local Nusselt number with dimensionless axial distance for $q = 241 \text{ W/m}^2$, $L_{calm.} = 60 \text{ cm}, q = 0^\circ$ (Horizontal).

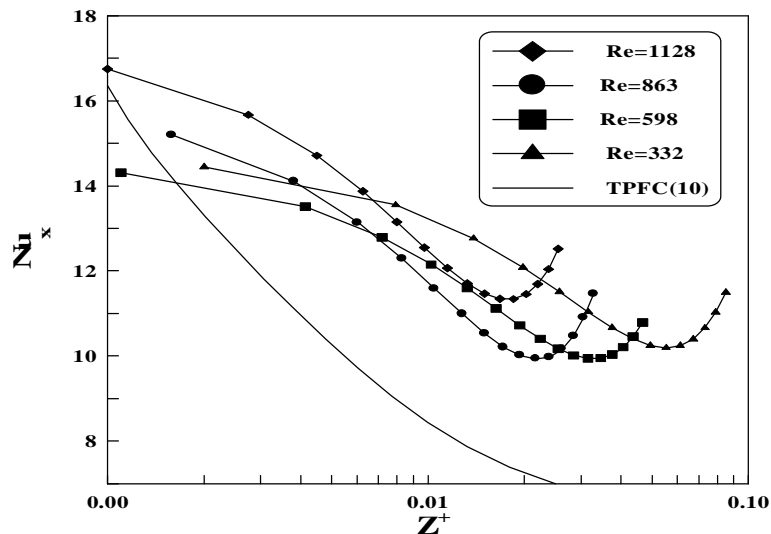


Figure (13). Variation of local Nusselt number with dimensionless axial distance for $q = 545 \text{ W/m}^2$, $L_{\text{calm.}} = 60 \text{ cm}$, $q = 0^\circ$ (Horizontal).

6. Conclusions

From the results obtained, the follow conclusions can be drawn:

1. The temperature profile along the annulus shows a steep profile near the heated surface.
2. Near the annulus entrance the velocity profiles for different heat flux were found to be similar to those for pure forced convection behavior. But in the annulus downstream the velocity profiles were distorted and a high degree of central concavity appeared by the action of buoyancy forces.
3. For high (Re) number, the velocity profiles does not change with the increase of heat flux, from the pure forced convection trend and no effect of buoyancy forces. But in low (Re) number the velocity profiles change with the increase of the heat flux.
4. The central concavity of velocity profiles diminishes as (x) increases but does not vanish completely. The degree of central concavity decreases as (Re) number increases.
5. The variation of (Nu_x) with (Z^+), was affected by many factors summarized in the as, heat flux, buoyancy force, Reynolds number.

7. References

- [1] Sha I., and Barnea Y., 1986, " Simple Analysis of Mixed Convection with Uniform Heat Flux ", *Int.J. Heat Mass Transfer*, Vol. 29, No.8,pp. 1139-1147.
- [2] Cony J., and El-Shaarawi M., 1975, "Finite Different Analysis for Laminar Flow Heat Transfer in Concentric Annuli with Simultaneously Developing Hydrodynamic and Thermal Boundary Layers ", *Int.J. For numerical methods in engineering*, Vol. 9, pp.17-38.
- [3] Chen Y., and Chung J.,1998, "Stability of Mixed Convection in a Differentially Heated Vertical Heated Vertical Channel ", *J. of Heat Transfer, Trans. of ASME*,Vol.120, pp. 127-132.
- [4] Hashimoto K., Akino N., and Kawamura H., 1986, "Combined forced -Free Convection Heat Transfer to A Highly Heated Gas in a Vertical Annulus". *Int.J.Heat Mass Transfer*, Vol.29, No.1, pp. 145-151.
- [5] Caampi M., Faggiani S., Grassi W., Incropera F.P., and Touni G., 1986, "Experimental Study of Mixed Convection in Horizontal Annuli for Low Reynolds Numbers ",*Int. Heat Transfer Conference 8th*, Vol. 3, pp. 1413-1418.
- [6] Zysina-Molozhen, L.M., Safonov, L.p., Zabezhinskiy, L.D., and Fel'dberg, L.A., 1973, " Heat Transfer by Combined Forced and Natural Convection in an Annulus Formed by Two Coaxial Cylinders ", *Heat Transfer-Soviet Research*, Vol.5, No.4.
- [7] Bohne, D., and Obermeier, E., 1986, "Combined Free and Forced Convection in a Vertical and Inclined Cylinder Annulus ", *Int. Heat transfer conference 8th oh*, Vol.3, PP.1401-1406.
- [8] Remash K. and Benjamin G., 1986, "Heat Transfer by Mixed Convection in a Vertical Flow Undergoing Transition ", *Int.J Heat Mass Transfer*, Vol.29, No. 8, pp. 1211 -1218.
- [9] Worsoe-Schmidt, P.M., 1967, "Heat Transfer in the Thermal Entrance Region of Circular Tubes and Annular Passages with Fully Developed Laminar Flow", *Int.J.Heat Mass Transfer*, Vol. 10, pp. 541 - 551.
- [10]Lundberg, R.E., Reynolds, W.C., and McCuen, P.A., 1962, "Heat Transfer in Annular Passages. General Formulation of the Problem for Arbitrarily Wall Temperature or Heat Fluxes ", *J. Heat Mass Transfer*, Vol. 6, pp. 438 – 439.
- [11]Huets, J., and Petit, J.P., 1974, " Natural and Mixed Convection in Concentric Annulus Space-Experimental and Theoretical Results for Liquid Metals", *Int. Heat Transfer conference 5th,Tokyo*, Vol. 3, PP.169-172.

- [12] Hanzawa, T., Sako, A., Endo, H., Kagawa, M., and Koto, K., 1986, " Combined Free and Forced Laminar Convective Heat Flux From Isothermally Heated Inner Tube in Vertical Concentric Annulus " J.Chem. Eng. Japan, Vol.97, pp.78-81.
- [13] Sherwin, K., and Wallis, J.D., 1972, " Combined Natural and Forced Laminar Convection for Upflow Through Heated Vertical Concentric Annuli ", Thermodynamics and Fluid Mechanics Conference, Inst.Mechanical Engineers, pp.1-5.

8 . Nomenclature

Symbol	Description	Unit
C_1, C_4	= Constants, eqs. (6)& (7)	-----
C_2, C_5	= Constants, eqs. (6)& (7)	$1/^\circ\text{C}$
C_3, C_6	= Constants, eqs. (6)& (7)	$1/^\circ\text{C}^2$
Cc_1, Cc_2, Cc_3	= Constants, eq. (8)	-----
Cc_4, Cc_5, Cc_6	= Constants, eq. (9)	-----
C_p	= Specific heat at constant pressure	$\text{J/kg.}^\circ\text{C}$
D_h	= Hydraulic diameter	M
G	= Gravitational acceleration	m/s^2
H	= Heat transfer coefficient	$\text{W/m}^2.^\circ\text{C}$
K	= Thermal conductivity	$\text{W/m.}^\circ\text{C}$
L	= Annulus length	m
M	= Radial mesh point in the annular space	-----
N	= Axial mesh point	-----
P	= Dimensionless pressure at any cross section = $p - p_i / \rho u_m^2$	-----
R	= Radial coordinate	m
r_1	= Inner radius of inner tube	m
r_2	= Outer radius of outer tube	

t_m	= Mixingcup temperature over any cross section	$^{\circ}\text{C}$
T	= Dimensionless temperature = $G.C_5(t - t_i)$	-----
T_A, T_B	= Constants	-----
U	= Axial velocity component	m/s
U_m	= Axial mean velocity	m/s
V	= Radial velocity component	m/s
V	= Dimensionless radial velocity component = v/u_m	-----
X	= Axial coordinate	m

Dimensionless Group

Re = Reynolds number $= r.v.D/m$

Superscript

a	Air
i	Annulus entrance (inlet)
s	Surface
t	Total
w	Wall
x	Local